

Sim2real transfer degrades non-monotonically with morphological complexity for flapping wing design

Kent Rosser

Defence Science and Technology
Group Australia
kent.rosser@dst.defence.gov.au

Jia Kok

Defence Science and Technology
Group Australia

Javaan Chahl

Dept. of Engineering and Math,
University of South Australia

Josh Bongard

Dept. of Comp. Sci.
University of Vermont

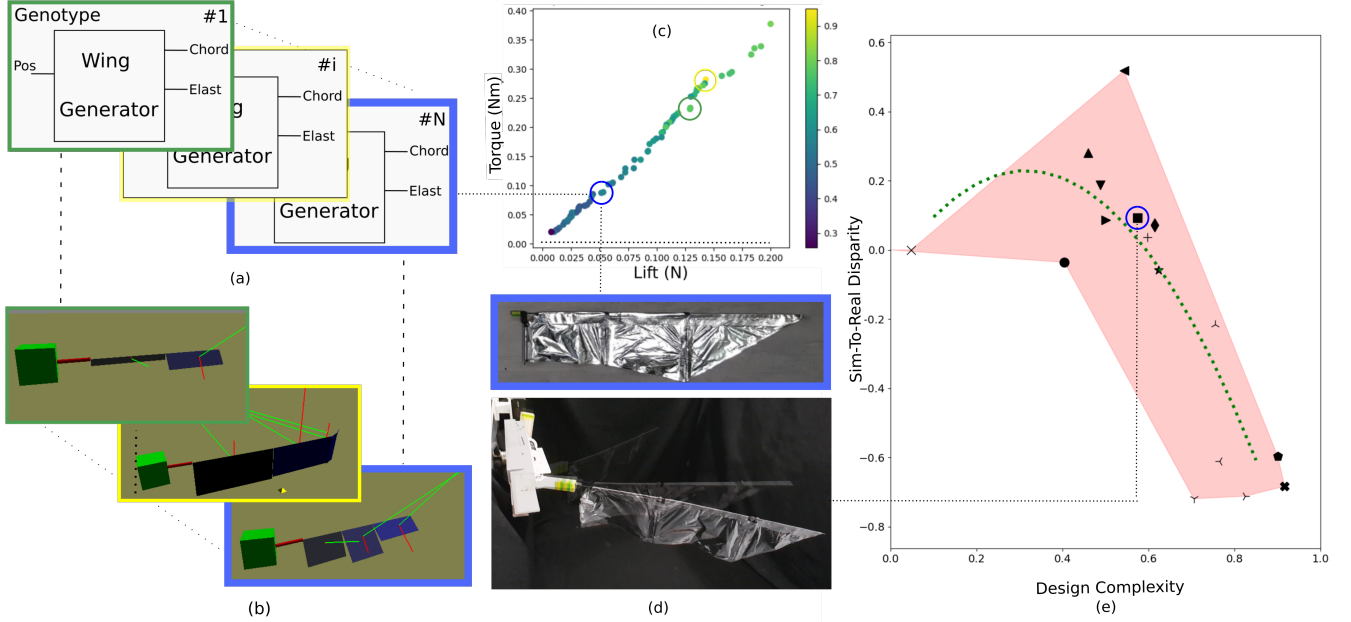


Figure 1. (a) population of wing descriptors ; (b) wing designs evaluated in simulation ; (c) Evolutionary algorithm produces optimal designs ; (d) individual undergo sim2real transfer ; (e) Scatter plot of sim2real gap

Abstract—We investigate the effect of morphology on sim2real transfer for flapping wing (FW) aerodynamics. By designing a set of aero-elastic wings suited to a constant control policy in simulation and transferring these to reality, we measure the shape of the sim2real gap as a function of morphological design complexity and find the relationship to be non-monotonic.

Keywords - sim2real ; morphology ; flapping wing

web: <https://youtu.be/xLpwg38TfRI>

I. AIMS

Morphology of a robot design is important to its ability to robustly achieve a stated goal [1, 6] and therefore applying machine learning approaches that include morphology as well as control in the design space provides scope for significant advantage as a holistic approach to robotics. Similar to development of control policies [8, 9, 7], morphology-in-the-loop design relies on the capability to design robots with differing morphologies in simulation [3] prior to performing sim2real transfer for assessment [12].

Our study is set in a domain known to be reliant on morphology - flapping wing flight [14]. We developed a parameterised morphology design space that draws key features from biologically evolved exemplars and we apply automated design methods to produce a set of high performance wing

morphologies in simulation. By performing sim2real transfer on a selection of these, for the first time we measure the shape of the sim2real gap for morphology-in-the-loop design. In doing so we introduce measures of sim2real difference and morphology simulation complexity, allowing us to consider the question of why some designs are more transferable than others without relying on post-hoc human interpretation.

II. METHODS

For this study, we produced a parameterised design descriptor for simulation evaluation as well as real world manufacture and test of a flapping wing test bed.

Key properties that are known to be important to the flight of natural fliers include wing shape, size and distribution of elasticity and inertia [11, 15]. Our approach includes the ability to specify each of these properties along the length of the wing within our bio-inspired parameterised design descriptor. That descriptor can then be interpreted into simulation and real world manufactured items.

We developed a cost-effective manufacturing method matched to the design descriptor shape, span, elasticity and inertia, and one example wing manufactured using this method is shown in Figure 1(c). Wings include a carbon fibre spar along the span of the physical wing. Chordwise elasticity along

the wing is discretized along the wing length by attaching ribs, oriented in the chordwise direction along the span of the wing, to the spar using spring elements made of stainless steel music wire of varying diameters for selectable levels of elasticity. An aerodynamic skin of aluminised mylar film is applied of the spar and ribs frame. A completed wing weighed $\sim 1\text{g}$, cost $\sim US\$1$ in parts and took ~ 1 hour to manufacture (plus cure).

A test rig (Figure 1(d)) actuates the wing and measures the mean lift achieved per flapping cycle using a load cell. For this experiment we defined a constant controller that oscillated the wing sinusoidally at 5Hz in 1 axis.

In variable morphology simulation, it is typical to model the design as a set of finite elements [12, 2, 4] and accumulate the localised effects experienced at each element to produce an overall performance. While much flapping wing research uses computational fluid dynamics for the analysis of a single design, those tools are poorly suited to evaluation of many different designs due to computation time, finite element meshing variation and fluid structural interaction.

For this study, we constructed our own finite element simulation capability suitable for flapping wing morphology assessment as a combination of physics engine [10] and quasi-static flapping wing aerodynamics [13]. Our simulation modelled a wing as a set of spanwise aligned, flat "blade" elements as shown in figure 1(b). Each blade embodied the quasi-static model to produce locally applied aerodynamic forces based on blade motion and properties. The rigid blades were connected by elastic joints allowing twist and bending of the wing under dynamic load within the simulator.

We created wing designs using an evolutionary method to select for designs that maximised lift per cycle while reducing drive power required. The best designs are shown in figure 1(c). In addition, we also produced three hand designs for comparison based on prior research studies [13, 5] converted to our parameterisation.

For our experiment, we took a set of designed wings and performed sim2real transfer. The metrics we used to analyse the sim2real gap for any design m are the sim2real transfer difference, STR , and morphology simulation complexity, C_S . STR is the normalised difference between simulation (\bar{L}_S) and real lift (\bar{L}_R) achieved (Equation 1). C_S is the normalised finite element implementation complexity of the simulator. As our simulator considered a wing as a set of blades where each blade inserts one quasi-static aerodynamic element of variable span and one elastic joint, we selected the accumulated span, $S(m)$, and number of blades $B(m)$ to represent its complexity (Equation 2). We normalise both STR and C_S using the maximum values transferred.

$$STR(m) = (\bar{L}_R(m) - \bar{L}_S(m)) / \bar{L}_{max} \quad (1)$$

$$C_S(m) = B(m) / B_{max} + S(m) / S_{max} \quad (2)$$

III. RESULTS

Wings that under went sim2real transfer are shown visually in Table I along with C_S , STR and \bar{L}_S and \bar{L}_R . Figure 1(e)




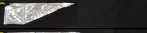
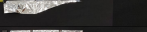
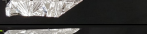










Wing	Design	C_S	\bar{L}_S (g)	\bar{L}_R (g)	STR
MIN		0.13	0.0	0.0 ± 0.1	0.0
CD-A		0.4	0.0	-0.5 ± 0.2	-0.04
CD-B		0.49	3.8	6.4 ± 0.1	0.19
EV-A		0.46	3.4	7.3 ± 0.3	0.28
EV-B		0.5	3.8	5.0 ± 0.4	0.09
EV-C		0.54	2.9	10.1 ± 0.7	0.52
EV-D		0.57	4.6	6.0 ± 1.0	0.1
EV-E		0.6	7.0	6.3 ± 0.1	-0.05
EV-F		0.61	5.2	6.2 ± 0.8	0.07
EV-G		0.62	8.0	7.2 ± 0.2	-0.06
EV-H		0.71	12.3	2.3 ± 0.4	-0.72
EV-I		0.75	5.4	2.4 ± 0.5	-0.22
EV-J		0.76	13.0	4.5 ± 0.2	-0.61
EV-K		0.82	13.1	3.2 ± 0.1	-0.71
EV-L		0.9	10.1	1.8 ± 0.1	-0.6
EV-M		0.92	13.9	4.4 ± 0.1	-0.68

Table I
SIM2REAL WING DESIGNS AND METRICS

shows the result as a scatter plot of $STR(m)$ versus $C_S(m)$. That plot includes a bounded region (shaded in pink) set by connecting the upper and lower bound of STR between adjacent transferred wings in the evolved search space. Overlaid on the plot is a polynomial line of best fit through the transferred points (green dashed line). The shape of the bounded region and line of best fit represents the empirically measured shape of the sim2real transfer gap for the flapping wing system.

IV. CONCLUSION

For the first time in this study, we have measured the shape of the sim2real gap that emerges during morphology-in-the-loop design as a function morphological simulation complexity. The shape in this instance shows the novel result that the relationship is non-monotonic. Up to a threshold complexity level of $C_S \approx 0.6$, real world behaviour of the robot under the sinusoidal control policy matches or even exceeds simulation. Above that threshold, STR quickly reduces resulting in the real performance of the robot being much worse than predicted.

The relationship we have found for the flapping wing problem using our reduced fidelity simulator shows that a rich search space of viable morphology solutions exists to be explored automatically up to the threshold level of C_S . The highest lift designs we found in reality were identified using evolution rather than hand design.

We specifically defined our complexity measure as a function of the finite element model rather than use post-hoc application of human explanations of specific modelling discrepancies. We believe that in future work, using this approach will assist in removing the need for human intuition in the selection of regions of the morphology space to search, as well as to identify regions for investment for model improvement.

V. ACKNOWLEDGEMENTS

We thank the support of the Defence Science and Technology Group Trusted Autonomy Systems Strategic Research Initiative and the Vermont Advanced Computing Core.

REFERENCES

- [1] Josh Bongard. Morphological change in machines accelerates the evolution of robust behavior. *Proceedings of the National Academy of Sciences*, 108(4):1234–1239, 2011.
- [2] Nicholas Cheney, Jeff Clune, and Hod Lipson. Evolved electrophysiological soft robots. In *ALIFE*, volume 14, pages 222–229, 2014.
- [3] Nick Cheney, Josh Bongard, Vytas SunSpiral, and Hod Lipson. Scalable co-optimization of morphology and control in embodied machines. *Journal of The Royal Society Interface*, 15(143):20170937, 2018.
- [4] Jack Collins, Wade Geles, David Howard, and Frederic Maire. Towards the targeted environment-specific evolution of robot components. In *Proceedings of the Genetic and Evolutionary Computation Conference*, pages 61–68. ACM, 2018.
- [5] GCHE De Croon, KME De Clercq, Remes Ruijsink, Bart Remes, and Christophe De Wagter. Design, aerodynamics, and vision-based control of the delfly. *International Journal of Micro Air Vehicles*, 1(2):71–97, 2009.
- [6] Martin Garrad, Jonathan Rossiter, and Helmut Hauser. Shaping behavior with adaptive morphology. *IEEE Robotics and Automation Letters*, 3(3):2056–2062, 2018.
- [7] Jemin Hwangbo, Joonho Lee, Alexey Dosovitskiy, Dario Bellicoso, Vassilios Tsounis, Vladlen Koltun, and Marco Hutter. Learning agile and dynamic motor skills for legged robots. *Science Robotics*, 4(26):eaau5872, 2019.
- [8] Nick Jakobi. Evolutionary robotics and the radical envelope-of-noise hypothesis. *Adaptive behavior*, 6(2): 325–368, 1997.
- [9] Sylvain Koos, Jean-Baptiste Mouret, and Stéphane Doncieux. The transferability approach: Crossing the reality gap in evolutionary robotics. *IEEE Transactions on Evolutionary Computation*, 17(1):122–145, 2013.
- [10] Sam Kriegman, Collin Cappelle, Francesco Corucci, Anton Bernatskiy, Nick Cheney, and Josh C Bongard. Simulating the evolution of soft and rigid-body robots. In *Proceedings of the Genetic and Evolutionary Computation Conference Companion*, pages 1117–1120. ACM, 2017.
- [11] Chengyu Li and Haibo Dong. Wing kinematics measurement and aerodynamics of a dragonfly in turning flight. *Bioinspiration & biomimetics*, 12(2):026001, 2017.
- [12] Hod Lipson and Jordan B Pollack. Automatic design and manufacture of robotic lifeforms. *Nature*, 406(6799):974, 2000.
- [13] Sanjay P Sane and Michael H Dickinson. The aerodynamic effects of wing rotation and a revised quasi-steady model of flapping flight. *Journal of experimental biology*, 205(8):1087–1096, 2002.
- [14] Wei Shyy, Hikaru Aono, Satish Kumar Chimakurthi, Pat Trizila, C-K Kang, Carlos ES Cesnik, and Hao Liu. Recent progress in flapping wing aerodynamics and aeroelasticity. *Progress in Aerospace Sciences*, 46(7): 284–327, 2010.
- [15] Bo Yin and Haoxiang Luo. Effect of wing inertia on hovering performance of flexible flapping wings. *Physics of Fluids*, 22(11):111902, 2010.